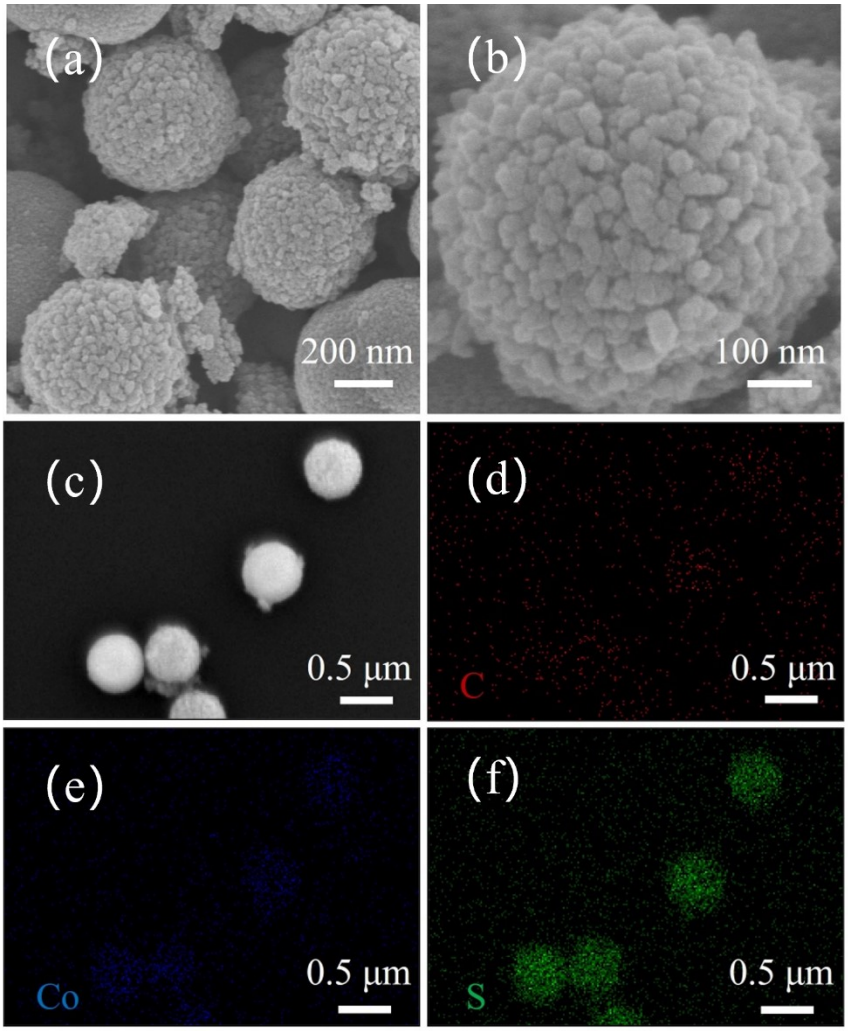


Fig S1. SEM of $CoS_2$@C at 450 °C (a, b) and corresponding elemental mapping images of S, C, Co (c, d, e, f)

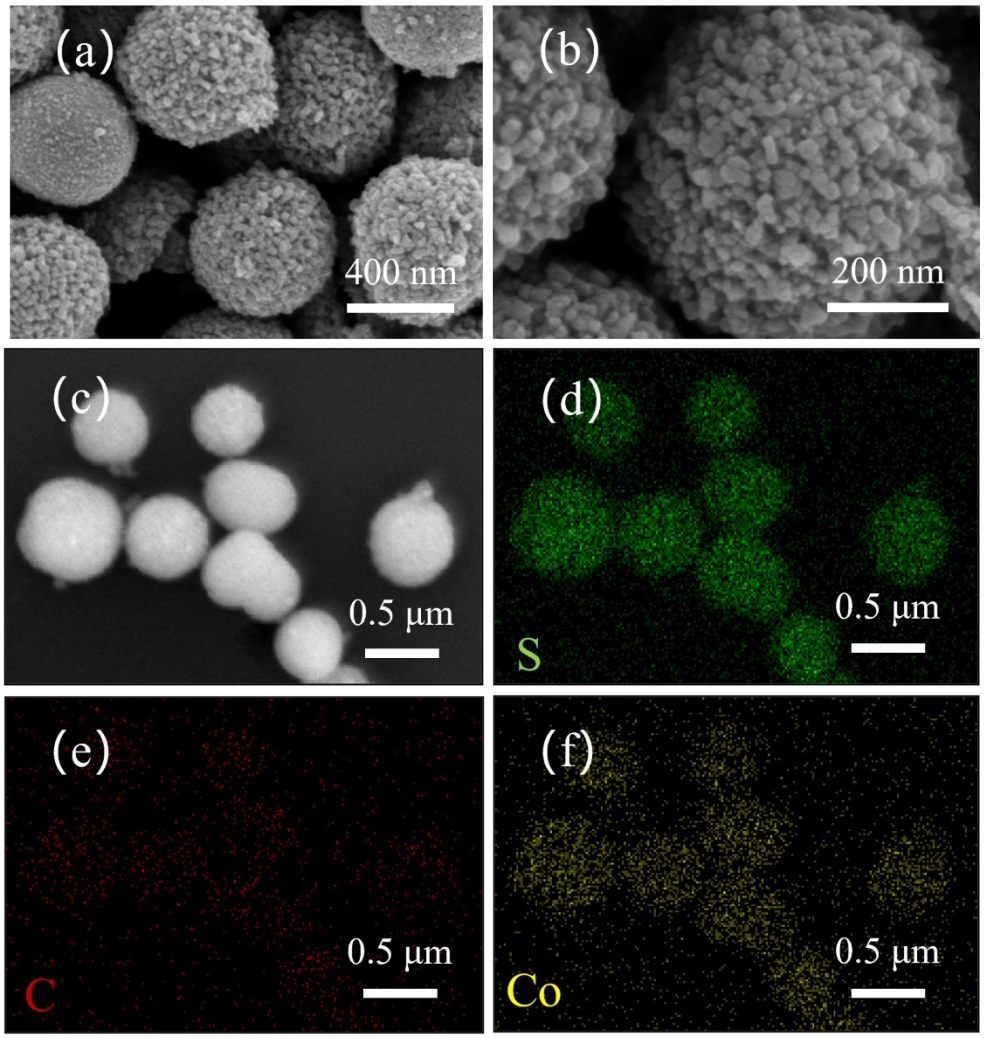


Fig S2. SEM of $CoS_2$@C at 550 °C (a, b) and corresponding elemental mapping images of S, C, Co (c, d, e, f)

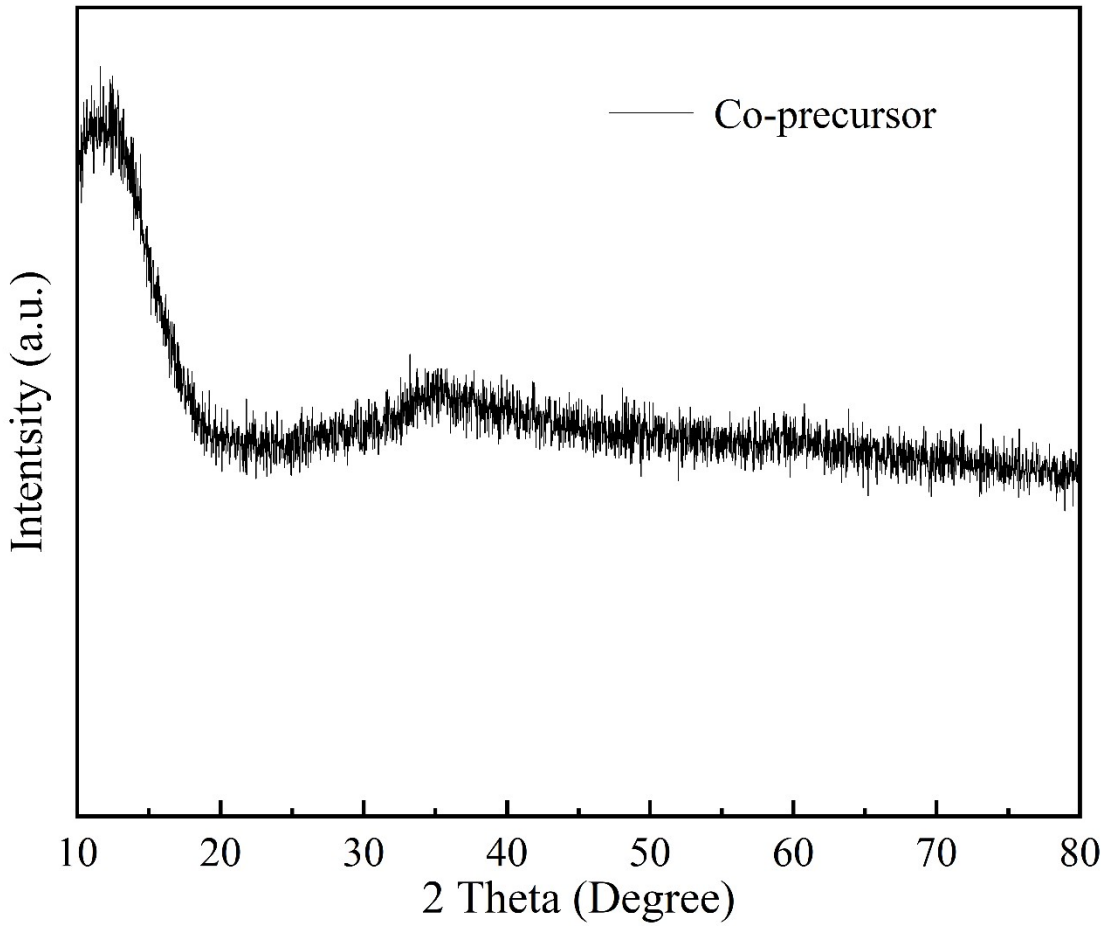


Fig S3. XRD patter of the cobalt-precursor

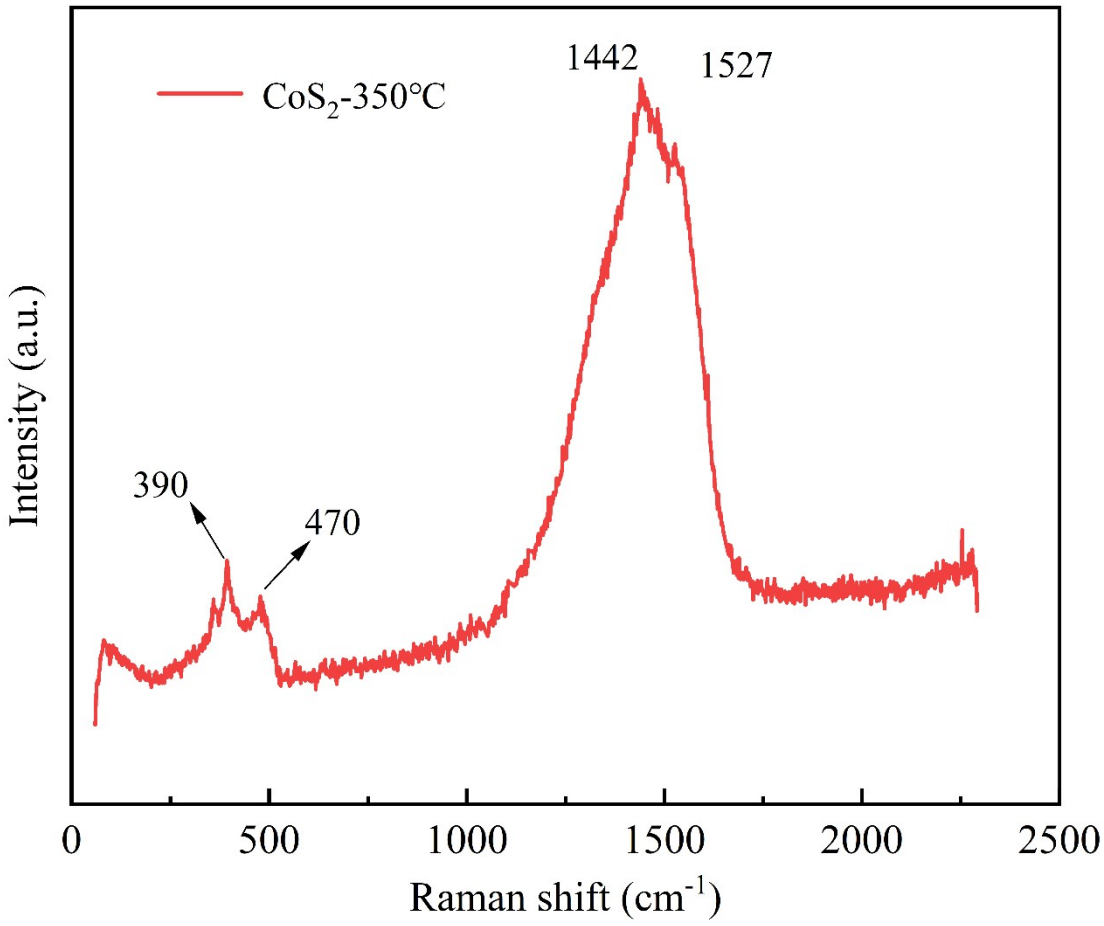


Fig S4. Raman image of $CoS_2$@C at 350 °C

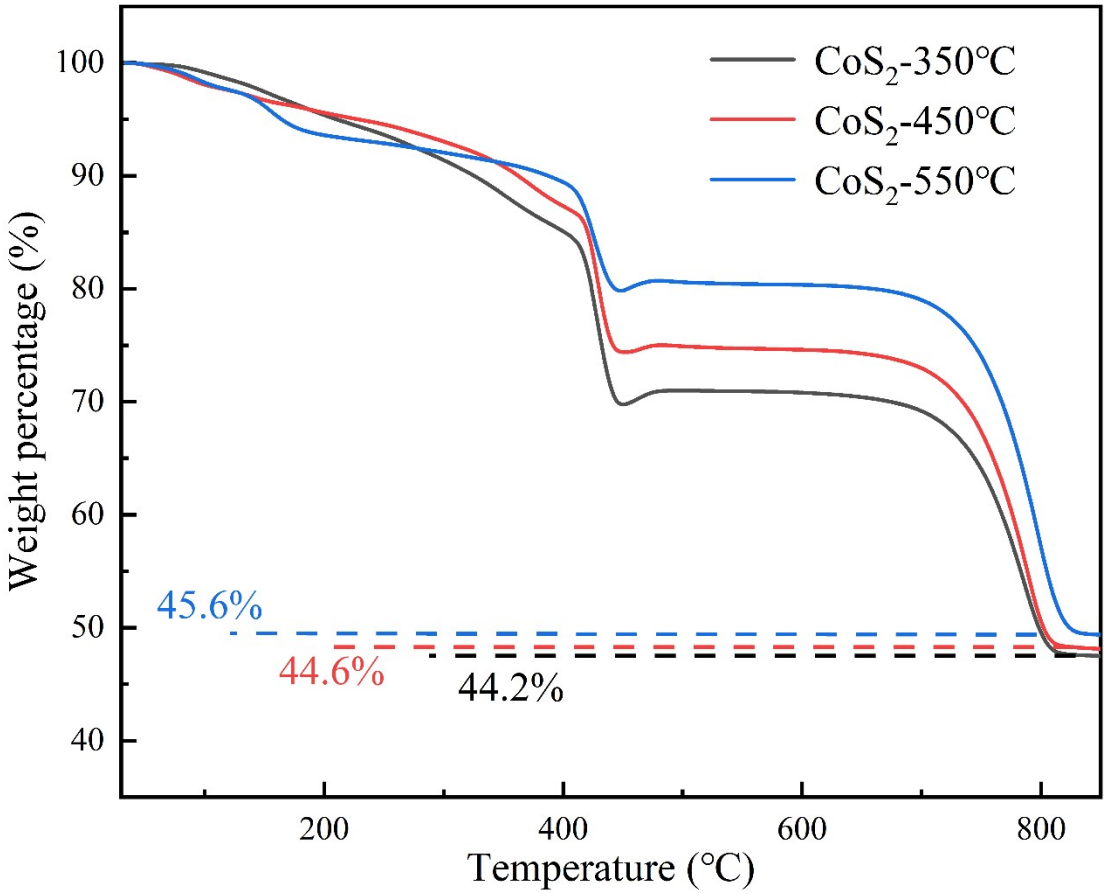


Fig.S5. TG curves of $CoS_2$@C at 350℃, 450℃ and 550℃ at a heating rate of 10 ℃ $min^{-1}$ in air.

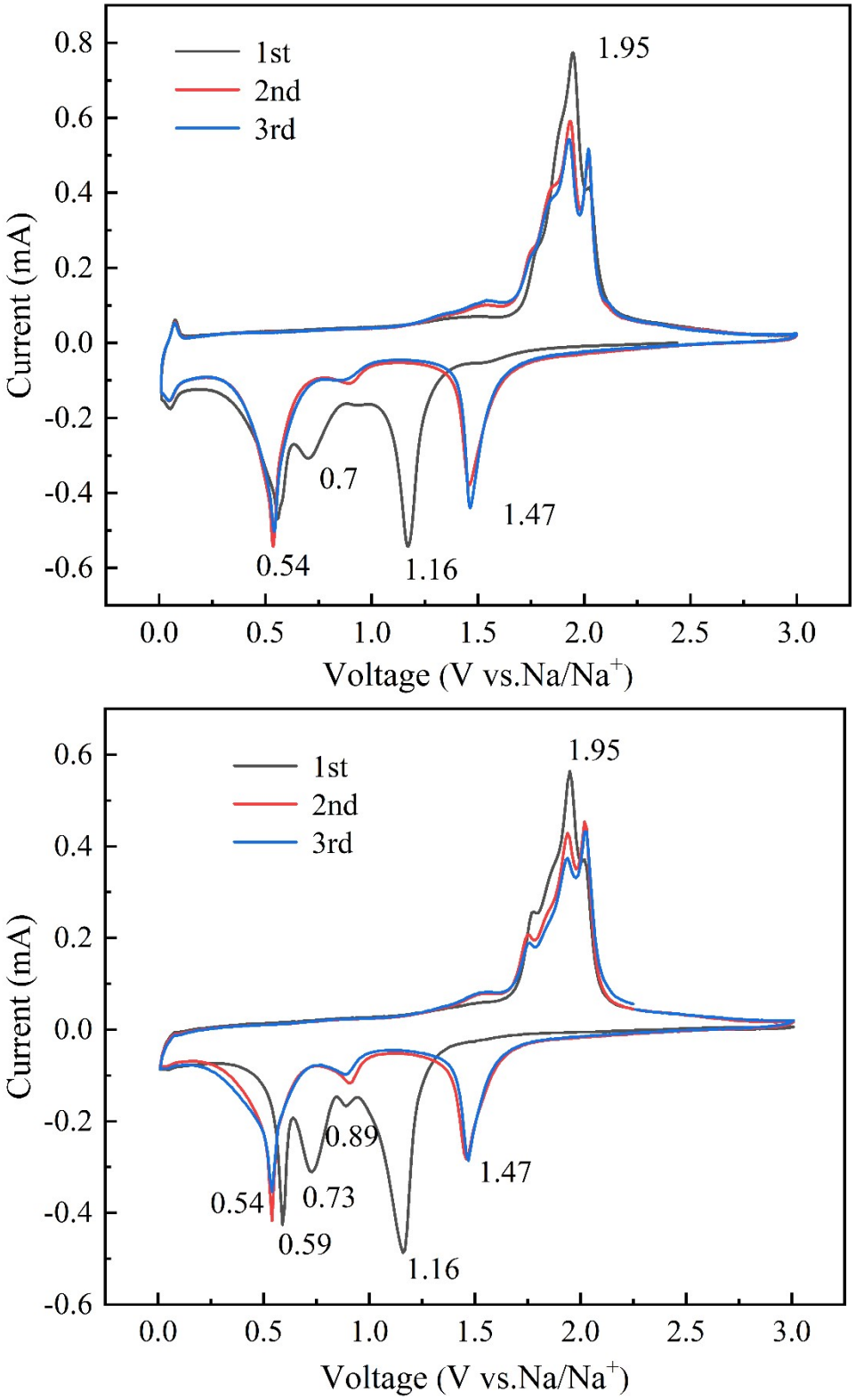


Fig S6. CV curves of $CoS_2$@C at 450 °C and $CoS_2$@C at 550 °C at a scan rate of 0.1 mV $s^{-1}$

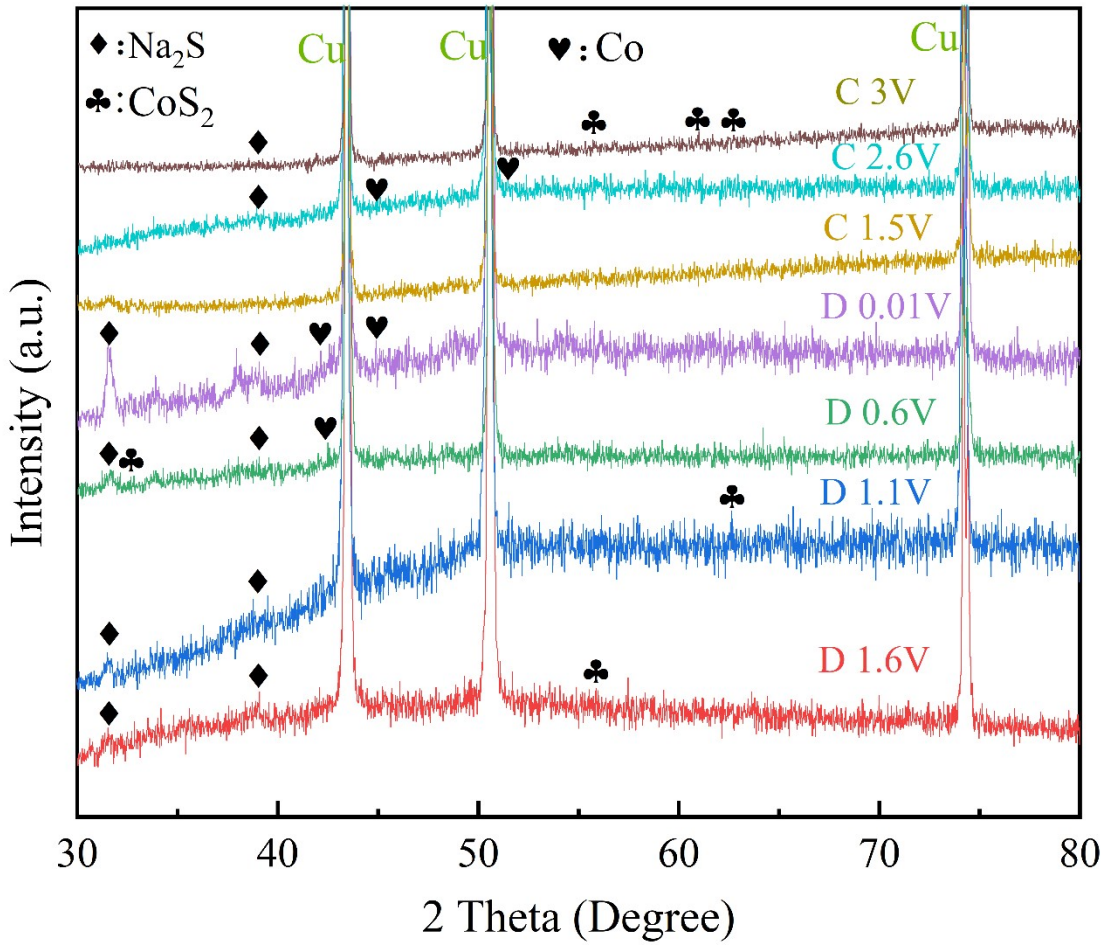


Fig S7. Ex-situ XRD patterns at different voltage states of $CoS_2$@C at 350 °C

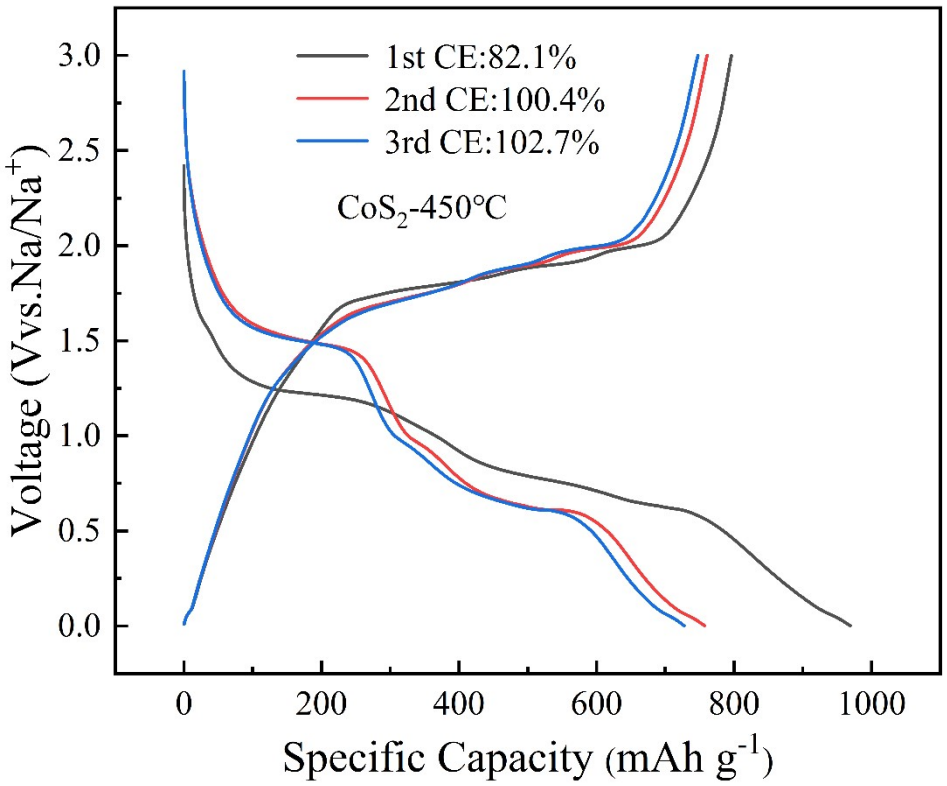


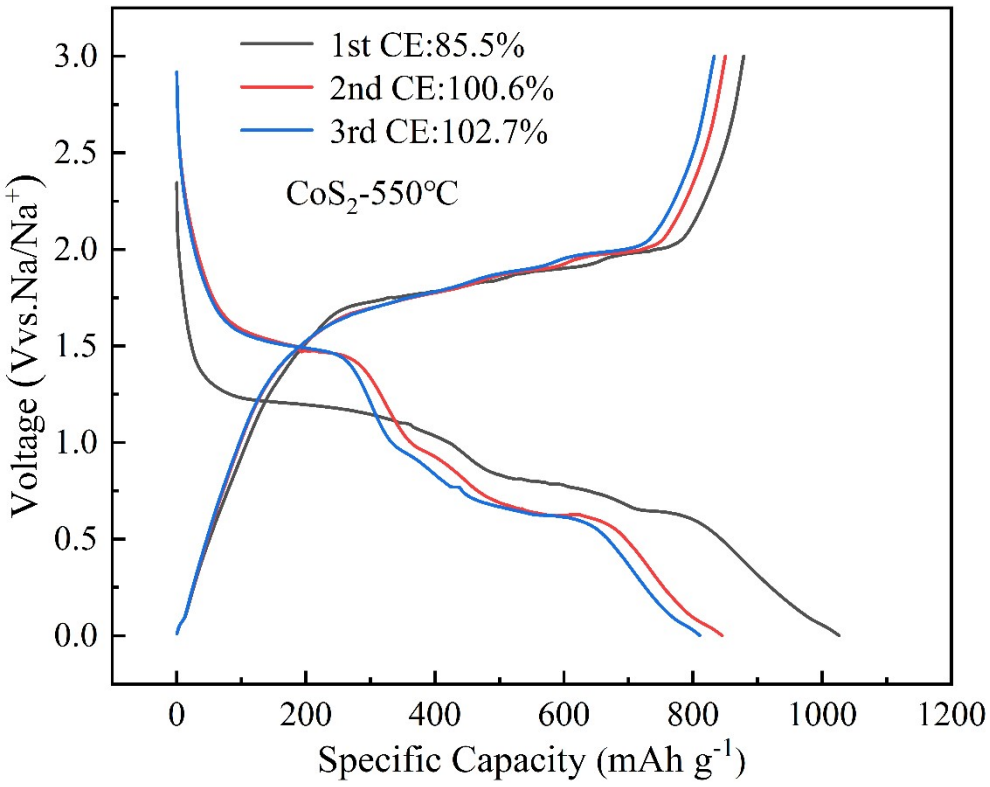


Fig S8. Discharge-charge curves of $CoS_2$@C at 450 °C, $CoS_2$@C at 550 °C for the first three cycles at 50 mA $g^{-1}$ current density

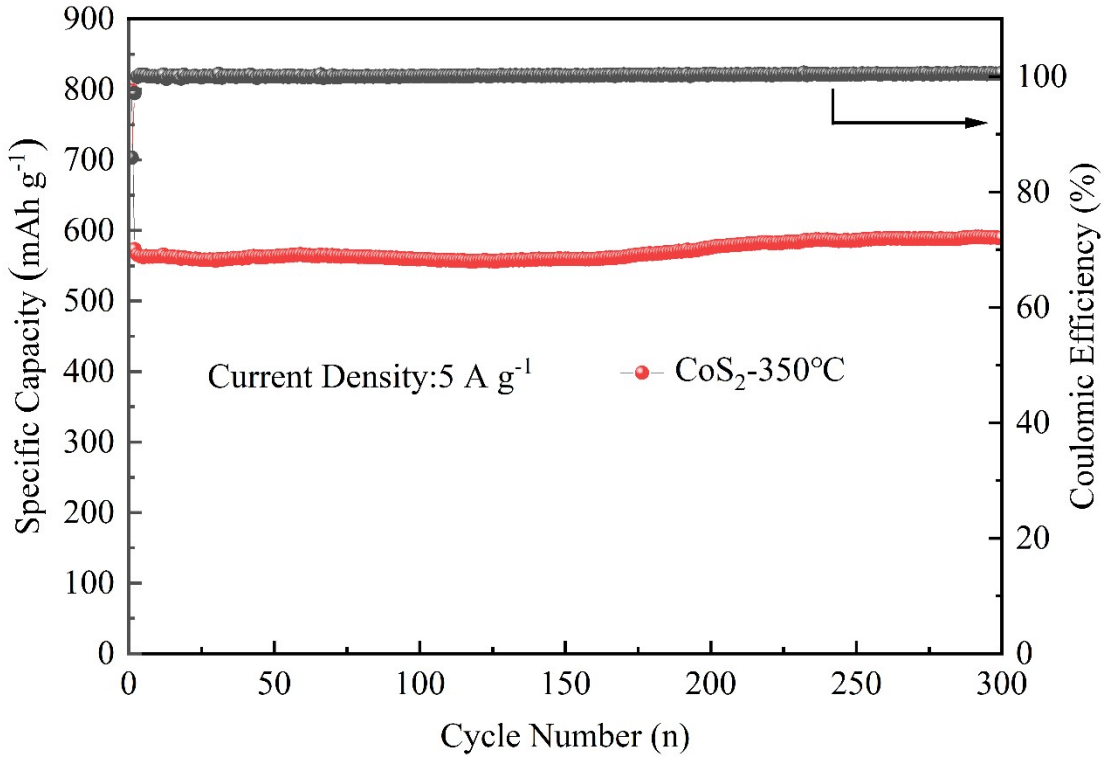


Fig.S9. Long-term cycling performance of $CoS_2$@C at 350℃ at 5 A $g^{-1}$

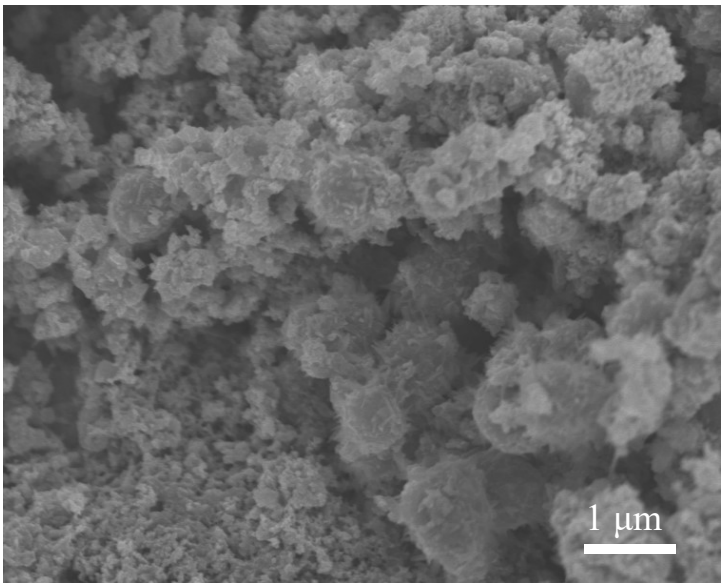


Fig S10. SEM image of $CoS_2$@C at 350 °C after cycles at current density of 2 A $g^{-1}$

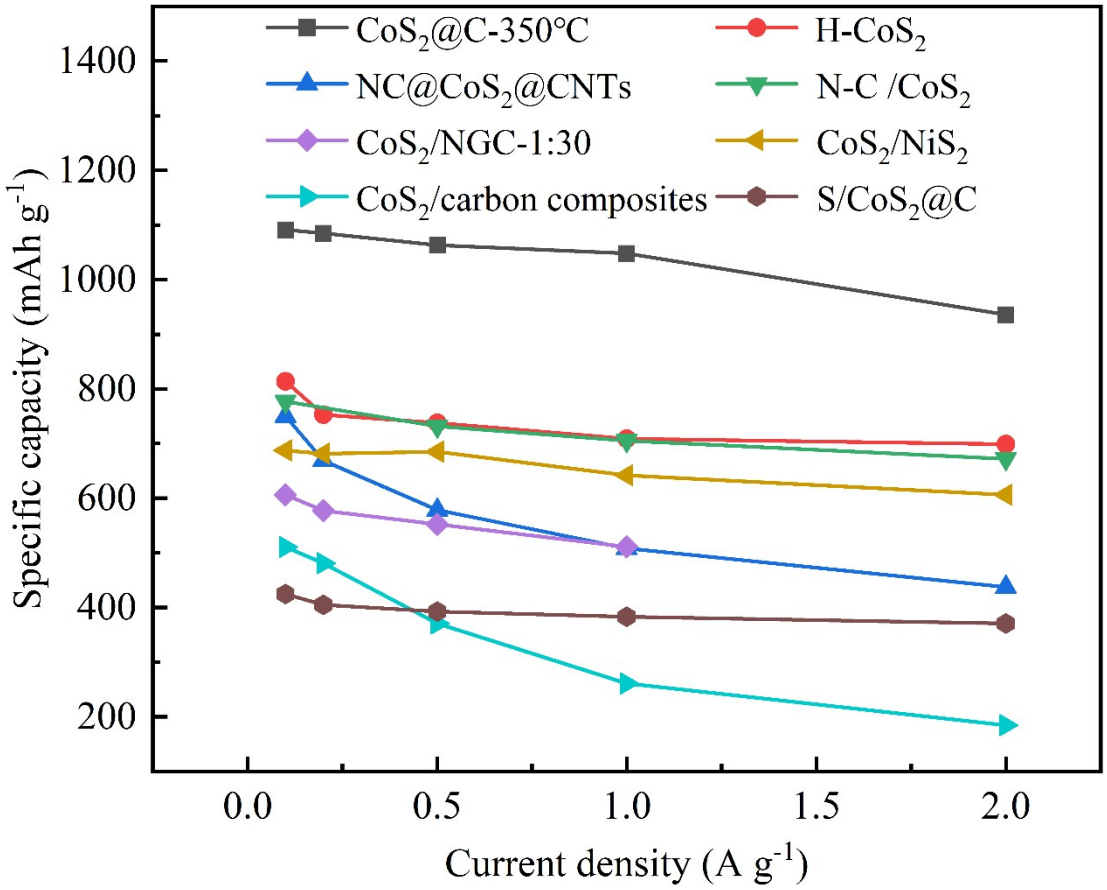


Fig S11. Comparison of the rate performance of the $CoS_2$@C at 350℃ electrode in our work and reported $CoS_2$-based composites

Table S1. Elemental analysis results for $CoS_2$@C -350 °C, $CoS_2$@C -450 °C and $CoS_2$@C -550 °C

| | C（%） | S（%） | Co（%） |
|---|---|---|---|
| $CoS_2$ -350℃ | 7.69 | 53.07 | 24.93 |
| $CoS_2$ -450℃ | 5.61 | 57.17 | 26.14 |
| $CoS_2$ -550℃ | 3.71 | 58.92 | 29.46 |